



Reinforced polydiphenylamine nanocomposite for microextraction in packed syringe of various pesticides

Habib Bagheri*, Zahra Ayazi, Ali Es'haghi, Ali Aghakhani

Environmental and Bio-Analytical Laboratories, Department of Chemistry, Sharif University of Technology, P.O. Box 11365-9516, Tehran, Iran

ARTICLE INFO

Article history:

Received 17 August 2011
Received in revised form
22 November 2011
Accepted 28 November 2011
Available online 6 December 2011

Keywords:

Polydiphenylamine/carbon nanotube nanocomposite
Microextraction in packed syringe
Multiresidue determination
Gas chromatography–mass spectrometry
Water analysis

ABSTRACT

Reinforced polydiphenylamine (PDPA) nanocomposite was synthesized by oxidation of diphenylamine in 4 molL⁻¹ sulfuric acid solution containing a fixed amount of carbon nanotubes (CNTs) in the presence of cetyltrimethylammonium bromide (CTAB). The surface characteristic of PDPA and PDPA/CNT nanocomposites was investigated using scanning electron microscopy (SEM). The prepared PDPA/CNT nanocomposite was used as an extraction medium for microextraction in packed syringe (MEPS) of selected pesticides from aquatic environment. The effect of CNT doping level and the presence of surfactant on the extraction capability of nanocomposite was investigated and it was revealed that when 4% (w/w) of CNT in the presence of CTAB is being used, the highest extraction recovery could be achieved. Eventually, the developed MEPS technique in off-line combination with gas chromatography–mass spectrometry (GC–MS) was applied to the analysis of some pesticides including triazine, organophosphorous, organochlorine and aryloxyphenoxy propionic acid pesticides. Important parameters influencing the extraction and desorption processes were optimized and a 25 cycles of draw–eject gave maximum peak area, when desorption was performed using 200 μL of n-hexane. Limits of detection (LODs) were in the range of 0.01–0.1 ng mL⁻¹ and 0.02–0.1 ng mL⁻¹ for distilled water and river water respectively, using time scheduled selected ion monitoring (SIM) mode. The method precision (RSD %) with four replicates was in the range of 1.6–14.6% for distilled water and 1.5–16.2% for river water at the concentration level of 5 ng mL⁻¹ while the linearity of method was in the range of 0.15–100 and 0.5–500 ng mL⁻¹. The developed method was successfully applied to different river water samples and the matrix factor for the spiked river water samples were found to be in the range of 0.74–1.09.

© 2011 Elsevier B.V. All rights reserved.

1. Introduction

Synthesizing nanostructured materials with novel and unique properties have attracted great attentions to design multifunctional structures at the nanometer scale. Nanocomposite can be considered as a multiphase solid material where one of the phases has nano-scale dimensions, or structures having nanometer-scale repeat distances between the different phases [1]. In overall, these materials possess different electrical, optical, mechanical, electrochemical, catalytic and structural properties in comparison with those of individual components. Due to their multifunctional behavior, any specific property of the nanocomposite is mostly more than the sum of the individual ones. The surface area/volume ratio of the reinforcing materials, a morphological characteristic, is a key issue for their spread applications [2].

CNTs, due to their combination of electrical and mechanical properties, are considered as the ideal reinforcing agents while their aggregation and agglomeration is still a major obstacle for the utilization of their technical potential. To overcome these problems, covalent attachment of CNTs with alkyl chains [3,4] and polymer/CNT composite preparation [5–11], based on non-covalent supra-molecular approach, are usually used. The polymer/CNT composite has been known to exhibit synergic effect [12,13]. However, due to their small size, CNTs are normally curled and twisted, and therefore the embedded CNTs in a polymer cannot show their complete potential. To maximize their reinforcing efficiency, the CNTs should be well dispersed to enhance the interfacial interaction with the matrix.

Conducting polymers (CPs) [14,15], mainly polypyrrole [16,17], polythiophene [18] and polyaniline [19,20], have been extensively used in many applications specifically in analytical chemistry [21,22]. However, not many reports on other CPs such as polydiphenylamine (PDPA) are available. Lately, PDPA has gained much attention due to its ease of processing and numerous applications [23–26].

* Corresponding author. Tel.: +98 21 66165316; fax: +98 21 66012983.
E-mail address: bagheri@sharif.edu (H. Bagheri).

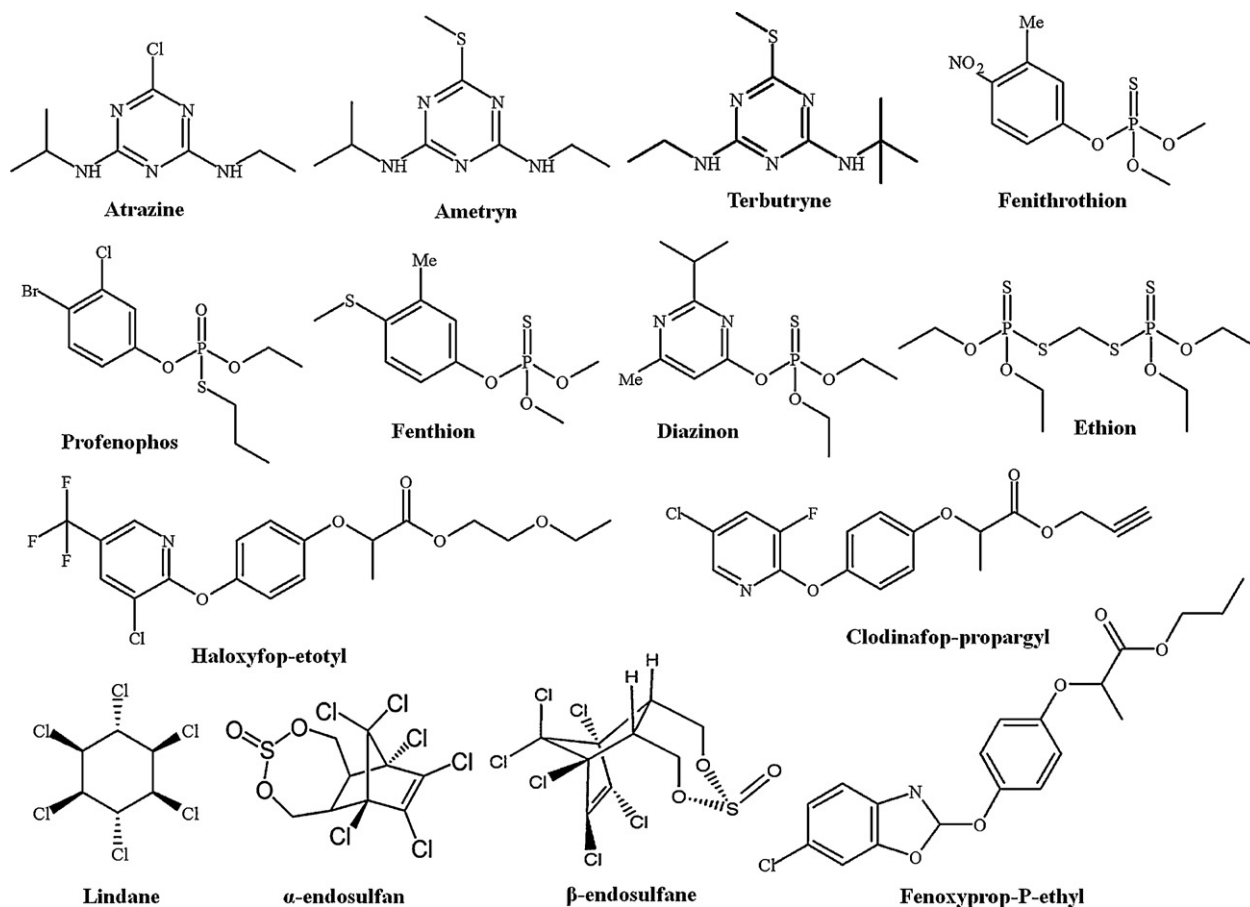


Fig. 1. Chemical structures of the selected analytes.

Microextraction in packed syringe is new miniaturized version of solid-phase extraction (SPE) in which sorbent amounts, sample volumes and desorption solvent volumes are minimized. In MEPS, the tinny sorbent material is inserted either into the barrel of a liquid handling syringe as a plug with polyethylene filters on both sides, or between the syringe barrel and the injection needle as a cartridge [27]. On-line combination of MEPS with a liquid chromatography (LC) [28,29] or a GC [30,31] can be achieved without any instrumental modification. Usually, the sample is drawn through the sorbent by an autosampler and the target analytes are adsorbed to the solid phase. The sorbent is then washed by water and/or acidic solution to remove the interfering material. Afterward, the analytes are eluted with an organic solvent or the LC mobile phase. MEPS has found more bio-oriented applications [27,29,32] and few reports concerning its use in environmental analysis could be found in the literature [30,33,34].

In this study an attempt was made to prepare PDPA/CNT nanocomposite in a way to obtain a PDPA polymer embedded with highly dispersed CNTs for achieving higher reinforcing efficiency. After successful preparation of PDPA/CNT nanocomposites with various CNT doping levels, they have been used as MEPS sorbent for the determination of some selected analytes from four major classes of pesticides.

2. Experimental

2.1. Reagents and standards

Triazines (atrazine, ametryn, terbutryn), organophosphorous pesticides (fenthion, fenitrothion, ethion, diazinon, profenophos),

organochlorine pesticides (lindane, α -endosulfan, β -endosulfan) were obtained from Merck (Darmstadt, Germany). Aryloxyphenoxy propionic acid pesticides including clodinafop-propargyl, haloxyfop-etotyl and fenoxaprop-P-ethyl were supplied from Dr. Ehrenstorfer GmbH (Augsburg, Germany), Dow AgroSciences (Indianapolis, USA) and Bayer CropScience (Monheim am Rhein, Germany) respectively. The chemical structure of selected analytes is shown in Fig. 1. The stock solution of these compounds was prepared in methanol at concentration of $1000 \mu\text{g mL}^{-1}$ and stored at 4°C . Methanol, ethanol, acetone, n-hexane, acetonitrile, hydrochloric acid (HCl), sodium hydroxide (NaOH), ammonium persulfate (APS), diphenylamine (DPA) and cetyltrimethylammonium bromide (CTAB) were obtained from Merck (Darmstadt, Germany). Multiwalled carbon nanotubes (MWCNTs) with purity higher than 95%, length of 1–10 μm and number of walls in the range of 3–15, was obtained from Plasma Chem GmbH (Germany).

2.2. Instrumentation

A gas chromatograph model Agilent 6820, with a split-splitless injection port and flame ionization detection (FID) system, was used to determine the optimized extraction conditions. Separation of analytes was carried out using a capillary column HP-1 MS (60 m \times 0.25 mm i.d.) with 0.25 μm film thickness (Hewlett-Packard, Palo Alto, CA, USA). The carrier gas was helium (99.999%) at a flow rate of 1 mL min^{-1} . The gas chromatograph was operated in the splitless mode and the split valve was kept closed for 1 min. The column was held at 100°C for 3 min, increased to 270°C at a rate of $70^\circ\text{C min}^{-1}$ and was kept at this temperature for 11 min. Then the temperature was raised to 290°C at $10^\circ\text{C min}^{-1}$ and was kept at

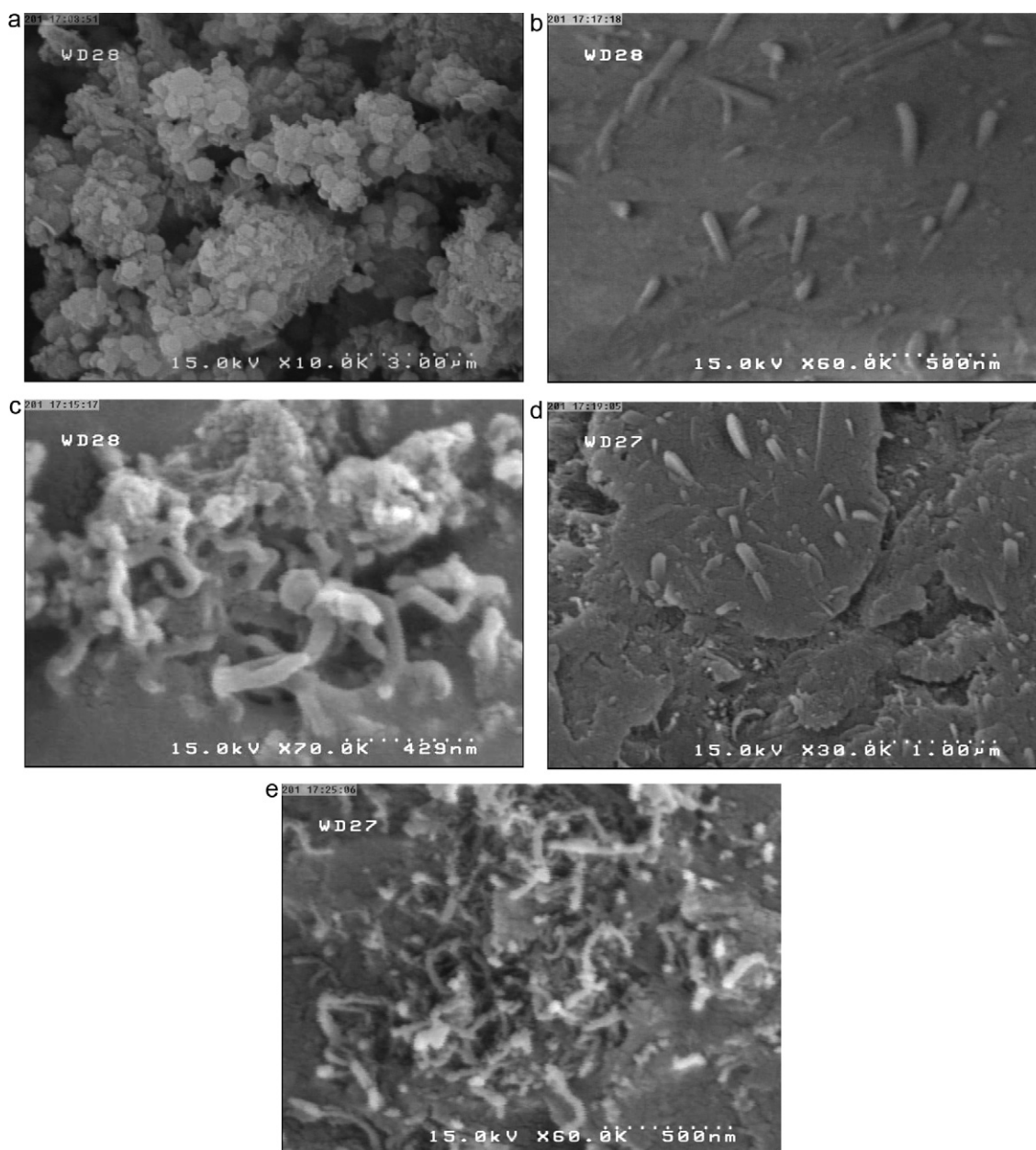


Fig. 2. SEM images of the prepared (a) bulk PDPA, (b) PDPA/CNT with CNT doping level of 3 mg, (c) PDPA/CNT with CNT doping level of 6 mg without CTAB, (d) PDPA/CNT with CNT doping level of 6 mg and (e) PDPA/CNT with CNT doping level of 12 mg.

this temperature for 7 min. The injector and detector temperatures were set at 200 and 290 °C respectively.

For quantitative determination, a Hewlett-Packard (HP, Palo Alto, USA) HP 6890 plus series GC equipped with a split-splitless injector and a HP 5973 mass-selective detector system were used. The MS was operated in the EI mode (70 eV). Helium (99.999%) was employed as carrier gas and its flow rate was adjusted at 1 mL min⁻¹. The separation of multiresidue pesticides was performed on a 30 m × 0.25 μm TRB-5 MS column (0.25 μm film thickness). The column was held at 100 °C for 3 min, increased to 220 °C at a rate of 30 °C min⁻¹ and was kept at this temperature for 3 min, then raised to 280 °C at 20 °C min⁻¹ and was kept at this temperature for 5 min. The injector temperature was set at 200 °C and the system was operated in the splitless mode for 1 min. The temperature of GC–MS interface, ion source and quadrupole was set at 280, 230 and 150 °C, respectively. The detection method was

programmed for SIM considering two or three characteristic ions for each compound.

In order to characterize the morphological properties of prepared nanocomposites the SEM images were obtained by a TESCAN VEGA II XMU (Berno, Czech Republic).

2.3. Preparation of PDPA/CNT nanocomposite

In a typical synthesis, 0.124 g CTAB and a fixed amount of CNTs (3, 6 and 12 mg) were added to 31 mL H₂SO₄ aqueous solution (4 mol L⁻¹) and sonicated for over 2 h to obtain well-dispersed suspensions. Then 0.146 g DPA was added to the suspension and it was sonicated for 20 min. Afterward a solution of H₂SO₄, 4 mol L⁻¹ (6.25 mL) containing 0.246 g ammonium persulfate was added sequentially to the suspension under stirring. The reaction mixture was stirred for 20 h at room temperature. The resulting dark green

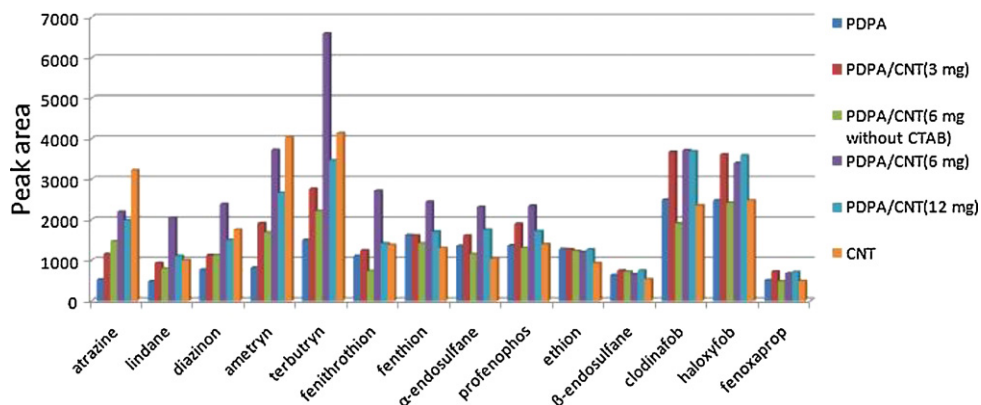


Fig. 3. Comparison of extraction capability of different prepared sorbents. Extractions were performed using 7 mL sample solution at concentration of $1 \mu\text{L mL}^{-1}$, with 50 cycles of draw-eject. Desorption was performed using 200 μL of acetonitrile.

Table 1
Amounts of reagents used in the PDPA nanocomposites synthesis.

PDPA/CNTs nanocomposite	DPA (g)	CNTs (mg)	CTAB (g)	APS (g)
A	0.146	3	0.124	0.246
B	0.146	6	0	0.246
C	0.146	6	0.124	0.246
D	0.146	12	0.124	0.246

precipitate was collected by filtration and rinsed with a solution of ammonia and then with distilled water for several times. The dark blue filtrate was then dried in oven at 50°C . In order to investigate the effect of surfactant on the synthesis process a nanocomposite with CNT doping level of 6 mg was prepared accordingly without adding CTAB. Also PDPA was prepared as discussed above without using CTAB and CNTs. Table 1 shows the quantity of the reagents used in the synthesis procedure of different nanocomposites.

2.4. MEPS condition

For these studies 1 mL insulin injection syringes were used. 2 mg of prepared sorbents was manually inserted inside the syringe between two polyethylene filters (SPE frits, $20 \mu\text{m}$ pore size). For this purpose the size of SPE frits have to be changed to match with used syringes. Before using for the first time, the sorbent was manually conditioned by rinsing with methanol, acetone and acetonitrile followed by 4 mL water. After that, spiked sample (7 mL) was drawn onto the syringe up and down several times using a variable speed

stirring motor which attached to a circular plate. Samples must be drawn with proportional speed to decrease the extraction time and to obtain good percolation between sample and solid support. In this work the speed of stirring motor was adjusted at 10 rpm ($170 \mu\text{L s}^{-1}$).

After performing the extraction, the syringe was dried under nitrogen flow for about 30 s and the analytes were then desorbed by 200 μL acetonitrile. The desorption step was performed by solvent aspiration into the syringe and then dispersion into desorption glass vial. Next, the desorption solvent was evaporated under N_2 flow until complete solvent drying. Finally 10 μL acetonitrile was added to the desorption vial and then 2 μL of desorbed solution was injected into the injection port of GC.

3. Results and discussion

3.1. PDPA/CNT nanocomposite

In order to synthesize PDPA/CNT nanocomposites, diphenylamine was oxidized in the presence of different amounts of CNTs. During the formation of PDPA/CNT, the chemical properties of CNT could not be affected by ongoing polymerization reaction, as they were only physically embedded into the network structure of PDPA. The surface characteristic of PDPA and PDPA/CNT nanocomposites was investigated using SEM (Fig. 2). The effectiveness of CNTs as a reinforcing filler in the polymeric matrix depends on (i) their content within the hosting

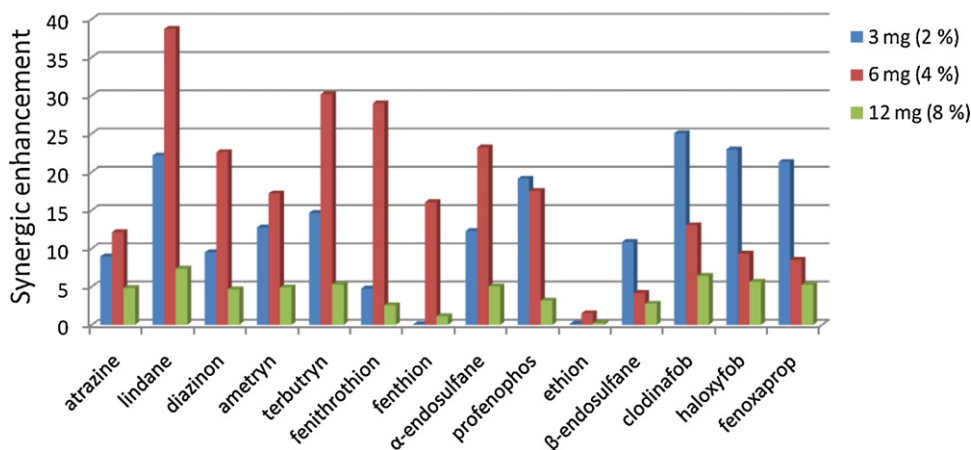


Fig. 4. Synergic effect for PDPA/CNT nanocomposites with different CNT doping levels.

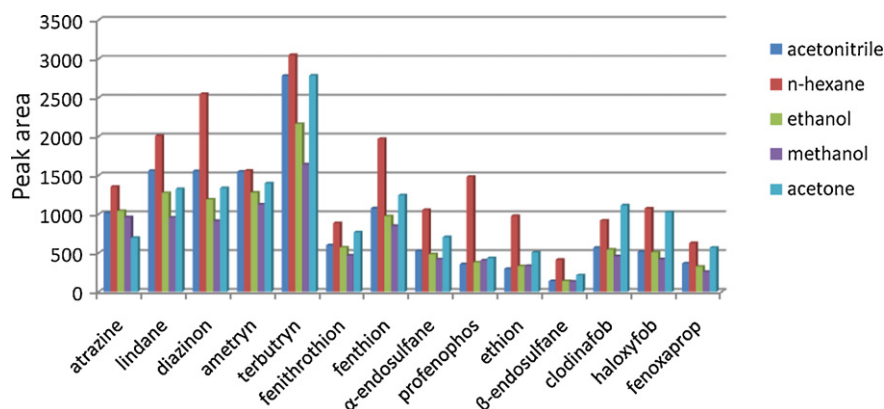


Fig. 5. Effect of desorption solvent on analytes responses. Extractions were performed using 7 mL sample containing analytes at level of $1 \mu\text{L mL}^{-1}$, with 50 cycles of draw-eject. Desorption was performed using 200 μL of various solvents.

system and (ii) the level of dispersion throughout the prepared nanocomposite. A non uniform CNTs dispersion can lead to many defect sites, limiting the efficiency of CNT as reinforcing filler [35–40]. Therefore, the surfactant addition and the CNTs doping level are among important features affecting the final structure of the prepared nanocomposite.

3.1.1. Effect of surfactant

The effect of surfactant on the nanocomposite extraction efficiency was studied and preliminary results revealed that presence of CTAB in the polymerization mixture could lead to the increased dispersion efficiency and higher extraction efficiency. As shown in Fig. 3 the PDPA/CNT synthesized with the CNT doping level of 4% (w/w) in the presence of CTAB (C) led to higher extraction capability compared to the same nanocomposite in which CTAB was excluded (B). The SEM images obtained from nanocomposite B (Fig. 2c) and nanocomposite C (Fig. 2d) revealed that in nanocomposite C higher CNTs dispersion is quite pronounced, while the aggregation of CNTs in the structure of nanocomposite B is rather observable.

Apparently when CTAB is used, CNTs are well dispersed in the primarily solution which leads to uniform dispersion of the embedded CNTs in PDPA. Surfactants can be adsorbed on the surface of CNTs through alkyl chain (hydrophobic segment) and the hydrophilic segment is stretched into water [41]. The surfaces of CNTs could be charged at the presence of the surfactant. Therefore the electrostatic repulsive forces between the surfactant molecules lead to the dispersion of CNTs in the aqueous solution under the sonication [42].

3.1.2. Effect of CNT doping level

For investigating the effect of CNT doping level on the PDPA/CNT extraction capability, three nanocomposites doped with 3, 6 and 12 mg of CNTs (2, 4 and 8%, w/w) were prepared. As shown in Fig. 3, the pristine CNTs and PDPA show low extraction capabilities in comparison with PDPA/CNT nanocomposites. These results revealed that the CNT doping level has an important role in the sorbent extraction ability. Apparently for most analytes, increasing the CNT doping level up to 6 mg leads to an improvement in extraction efficiency, while after that the trend takes a different path which might be due to agglomeration of CNTs bundles [42–44]. The SEM images of nanocomposites with the CNT doping level of 3 mg (A), 6 mg (C) and 12 mg (D) are shown in Fig. 2b, d and e, respectively. The aggregation of CNTs is seen in D which subsequently leads to lower extraction capability. According to these results the CNTs doping level of 6 mg was chosen as the optimum value.

The synergic enhancement (SE) in extraction efficiency can be defined as the resulted extraction recovery changes over expected extraction recovery change.

$$SE = \frac{R_{PDPA/CNT} - R_{PDPA}}{W_f \times R_{CNT}} \quad (1)$$

where $R_{PDPA/CNT}$, R_{PDPA} and R_{CNT} are the extraction recovery obtained when PDPA/CNT nanocomposite, PDPA and CNT, were used as the extracting medium. The W_f term represents the mass fraction of CNT in the nanocomposite. The synergic effect for different PDPA/CNT nanocomposites containing various amounts of CNT was calculated using Eq. (1). As shown in Fig. 4 the synergic effect for PDPA/CNT nanocomposite with the doping level of 6 mg (C) is prominent for nine analytes, while for the rest of them the synergic effect of the nanocomposite with the doping level of 3 mg (A) is quite distinctive.

Considering Fig. 4 one can conclude that the synergic enhancement for extraction capability of the synthesized nanocomposite depends not only on the CNT doping level but also the structure and properties of the analytes. Various mechanisms such as π - π interactions, hydrogen bonds, hydrophobic and electrostatic interactions might be simultaneously involved when organic compounds–CNTs interactions are concerned. Generally in π - π interactions the size and shape of the aromatic system along with the substitution units of the molecule are major key players [45–47]. It has been shown that both electron-withdrawing ($-\text{NO}_2$ and $-\text{Cl}$) and electron-donating ($-\text{NH}_2$ and $-\text{OH}$) substituents on benzene could enhance the adsorption of molecules on CNTs [48,49]. Our investigations revealed that aryloxyphenoxypenic acid pesticides exhibit the highest synergic effect when the prepared nanocomposite contains 3 mg of CNTs doping level (Fig. 4). According to structures of the selected analytes (Fig. 1), this could be due to the presence of more aromatic rings on these molecules. But by increasing the CNTs doping level, the extraction efficiency of aryloxyphenoxypenic acid pesticides remained almost the same and their relevant synergic effects were reduced as W_f was increased (Eq. (1)). In case of organophosphorous pesticides the synergic effect was changed in the order of fenitrothion > diazinon > profenophos > fenthion > ethion. Contributions of different substituents on each compound could be the major criteria for this order. As it has been shown [50] the adsorption affinity of aniline and phenol on CNTs with different substituted groups has been increased with the following order: nitro group > chloride group > methyl group. Fenitrothion has shown to have the highest synergic effect which might be related to the presence of nitro groups on the aromatic ring. Ethion with no aromatic rings and

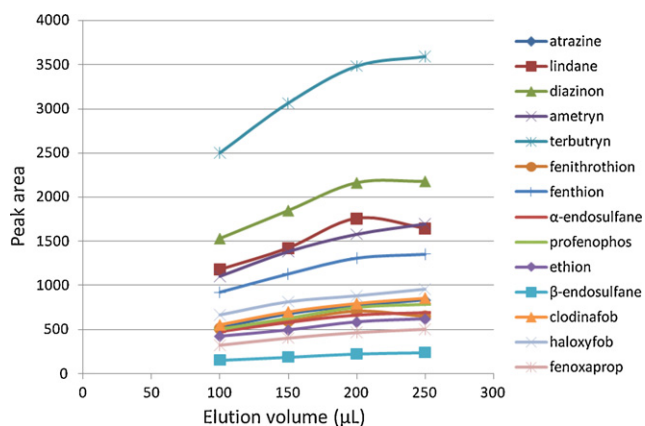


Fig. 6. Effect of elution volume on analytes peak area. Extractions were performed using 7 mL sample containing analytes at level of $1 \mu\text{L mL}^{-1}$, with 50 cycles of draw-eject. Desorption was performed using various volumes of n-hexane.

any influential substituent in its chemical structure is expected to have the lowest synergic effect. For triazines, the synergic effects were in the order of terbutryn > ametryn > atrazine. Although other factors can affect the synergic enhancement but the number of methyl groups in these compounds seems to have a dominant role. In the case of organochlorine compounds lindane, a strong electron withdrawing compound, exhibits the highest synergic effect.

3.2. Optimization

3.2.1. Desorption condition

The influence of both desorbing solvent and its volume were investigated, to ensure effective elution of the trapped analytes from the sorbent. The elution solvent should be able to displace the target analytes from the sorbent at the lowest possible volume. If the retention is based on hydrophobic interactions only, non-polar solvents can disrupt the binding forces among the analytes and the sorbent. Different organic solvents with various functionality and polarity were used to investigate the optimum desorption condition. The extraction was performed using 7 mL of aqueous sample spiked with the target analytes at a concentration level of $1 \mu\text{g mL}^{-1}$, when the pump cycles was set at 50 (10 rpm) and 200 μL of desorbing solvent was used. As shown in Fig. 5 n-hexane exhibited the highest desorption efficiency and was therefore chosen as desorption solvent for further experiments. In this study the effect of desorbing solvent volume was also investigated (Fig. 6).

The analytes responses were enhanced as eluting solvent volume was increased up to 200 μL and remained constant after this point. Therefore a solvent volume of 200 μL was chosen for the elution of analytes.

3.2.2. Draw-eject cycles

In MEPS it is possible to draw the sample through the sorbent located inside the syringe, once or several times (draw-eject). The multiple extraction cycles can be achieved by draw-eject of a fraction of sample in the same vial or by drawing up from aliquot of sample and discarding it in the waste (extract-discard mode). In this study the influence of extraction cycles (draw-eject) on the extraction efficiency was evaluated. Multiple draw-eject of the sample in the same vial was preferred to extract the selected analytes from 7 mL water samples [30,51]. It was shown that the maximum extraction yield for all analytes was achieved after 25 pump cycles. After this point the analytes responses remained rather constant and no enhancement in responses was observed. Furthermore, for investigating the efficiency of extract-discard mode, this procedure was applied to the extraction of 7 mL of sample with an analyte concentration of $1 \mu\text{g mL}^{-1}$ by draw-discarding 1 mL of sample to another vial. Therefore in order to draw whole sample it was necessary to repeat this cycle for 7 times (7×1). For extraction of whole sample for n times it is essential to use $7 \times 1 \times n$ protocol. Considering the obtained results, all analytes' responses were rather enhanced with increasing n from 1 to 2, but its further increase led to insignificant changes in analytes' responses. The extract-discard mode in comparison with draw-eject in a same vial using 25 cycles has led to any improvement in extraction efficiency. Thus, considering the simplicity of draw-eject in a same vial and use of automation for extractions, 25 cycles of draw-eject in a same vial was selected for the further extractions.

3.2.3. Effect of sample pH

The sample pH is a significant factor, which could affect the analytes extraction recovery from water samples. Considering the optical sensing of pH by PDPA ($\text{pK}_a = 8.70$) [23], the effects of pH on the extraction efficiency of the selected analytes from water samples were evaluated at the pH interval of 2–11. As shown in Fig. 7, the extraction efficiency of PDPA/CNT nanocomposite for most analytes was increased when the sample pH was raised to 5. In overall, the extraction at pH 5 was found to be the most suitable condition. These results can be easily described considering the acid–base equilibrium of PDPA in the solutions having different pH values. The extraction capability of PDPA depends on the intermolecular interactions such as acid–base, π – π , dipole–dipole, and

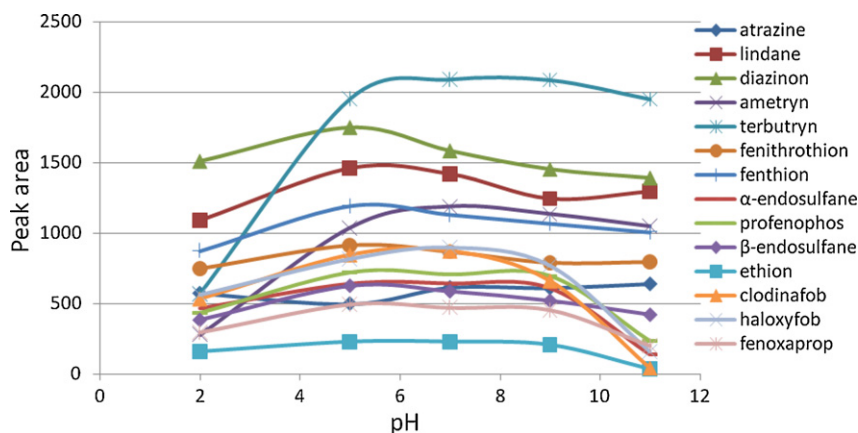


Fig. 7. Effect of pH on the extraction efficiency. Extractions were performed using 7 mL sample containing analytes at level of $1 \mu\text{L mL}^{-1}$, with 25 cycles of draw-eject. Desorption was performed using 200 μL of n-hexane.

Table 2

Some analytical data obtained after MEPS of selected analytes from distilled water sample using the CNT/PDPA nanocomposite and GC–MS.

Compound	Retention time (min)	LOD ^a (ng mL ⁻¹)	LDR ^b (ng mL ⁻¹)	R ²	RSD ^c % (n=4)	AR ^d (%)	EF ^e
Atrazine	8.48	0.01	0.5–200	0.9950	14.6	36	254
Lindane	8.72	0.05	0.5–200	0.9992	6.9	57	401
Diazinon	8.79	0.05	0.5–200	0.9989	4.5	91	634
Ametryn	9.69	0.05	0.5–200	0.9969	5.5	78	550
Terbutryn	10.01	0.07	0.5–500	0.9996	3.8	59	410
Fenitrothion	10.09	0.05	0.5–100	0.9900	2.7	87	612
Fenthion	10.44	0.05	0.5–200	0.9905	1.6	74	519
α-Endosulfan	11.73	0.07	0.35–350	0.9897	4.5	68	472
Profenophos	12.01	0.1	0.5–200	0.9924	3.1	85	592
β-Endosulfan	12.64	0.015	0.15–100	0.9831	6.2	54	378
Ethion	12.73	0.05	0.5–500	0.9832	7.58	75	523
Clodinafop-propargyl	13.14	0.01	0.5–200	0.9924	8.2	104	731
Haloxypop-etotyl	13.48	0.05	0.5–200	0.9895	3.7	101	705
Fenoxypop-P-ethyl	15.30	0.01	0.5–100	0.9883	5.0	74	516

^a Limit of detection.^b Linear dynamic range.^c Relative standard deviation.^d Absolute recovery.^e Enrichment factor.

ion exchange which might occur between PDPA and analytes. Since PDPA is positively charged in acidic media, the interaction with analytes could be reduced. At higher sample pH, the positive charges on PDPA are reduced and the attractive inter-molecular interactions between analytes and PDPA become more dominant, therefore, the extraction efficiency is expected to be increased.

3.3. Method validation

Based on the method development observed above, n-hexane as desorption solvent, elution volume of 200 μL, pH = 5, 25 cycles of draw-eject in a same vial were selected for the determination of selected analytes in water. Double distilled water and Ghezal-ouzan river (East Azarbayjan province-Iran) spiked with the selected analytes were used to evaluate the precision of the measurements, the limits of detection and the dynamic range of the method. The linearity of the method was studied by preparing the calibration curve for each analyte. Considering the distilled water samples, the obtained calibration graphs for most of analytes were linear in the concentration range of 0.5–200 ng mL⁻¹, but for terbutryn and ethion the linearity was in the range of 0.5–500 ng mL⁻¹. The calibration curves obtained for β-endosulfan, α-endosulfan and fenoxypop-P-ethyl showed the linearity range of 0.15–100 ng mL⁻¹, 0.35–350 ng mL⁻¹ and 0.5–100 ng mL⁻¹, respectively (Table 2). The regression coefficient for the analytes was rather satisfactory (R² > 0.9831). For river water sample, the calibration graphs were linear in the range of 0.5–100 ng mL⁻¹ for most of analytes

except lindane and ethion (0.5–500 ng mL⁻¹), fenthion and profenophos (0.5–200 ng mL⁻¹), β-endosulfan (0.15–100 ng mL⁻¹) and α-endosulfan (0.35–350 ng mL⁻¹). The regression coefficient for all analytes was greater than 0.9824. LODs based on a signal-to-noise ratio of 3/1, for distilled water were in the range of 0.01–0.1 ng mL⁻¹ (Table 2) and for river water were in the range of 0.20–0.1 ng mL⁻¹ using SIM mode (Table 3).

Absolute recoveries (AR) were determined by comparison of the response obtained by MEPS of 7 mL of sample at 5 ng mL⁻¹ versus the response of a direct injection of 2 μL of a 1 μg mL⁻¹ standard solution. Results for distilled water ranged from 68% to 104%, except for atrazine, lindane, terbutryn and α-endosulfan (Table 2) and for river water ranged from 61% to 82% except for atrazine, terbutryn and β-endosulfan (Table 3). Enrichment factors for all analytes were calculated and reported in Tables 2 and 3.

The method reproducibility was evaluated by performing four consecutive extractions from the aqueous solution. The RSD % was ranging from 1.6% to 14.6% at 5 ng mL⁻¹ for distilled water and from 1.5% to 16.2% for real water sample. The potential for carryover of analytes was investigated by desorption of washed MEPS syringe after extraction of a spiked sample solution at level of 5 ng mL⁻¹. There were no peaks above baseline at the corresponding retention times for each analyte.

3.4. Matrix effect and real water sample analysis

To evaluate the applicability of the developed method, water samples obtained from Zayandeh-roud river (Isfahan-Iran),

Table 3

Some analytical data obtained after MEPS of selected analytes from Ghezal-ouzan river sample using the CNT/PDPA nanocomposite and GC–MS.

Compound	Retention time (min)	LOD (ng mL ⁻¹)	LDR (ng mL ⁻¹)	R ²	RSD % (n=4)	AR (%)	EF
Atrazine	8.48	0.05	0.5–100	0.9918	16.2	27	187
Lindane	8.72	0.05	0.5–500	0.9977	4.7	61	425
Diazinon	8.79	0.03	0.5–100	0.9960	7.5	77	537
Ametryn	9.69	0.1	0.5–100	0.9965	12.8	63	444
Terbutryn	10.01	0.1	0.5–100	0.9974	6.5	48	335
Fenitrothion	10.09	0.02	0.5–100	0.9951	8.4	78	546
Fenthion	10.44	0.1	0.5–200	0.9896	1.5	65	455
α-Endosulfan	11.73	0.1	0.35–350	0.9976	8.2	69	483
Profenophos	12.01	0.1	0.5–200	0.9963	3.8	76	535
β-Endosulfan	12.64	0.02	0.15–100	0.9824	2.2	53	373
Ethion	12.73	0.1	0.5–500	0.9832	15.2	82	570
Clodinafop-propargyl	13.14	0.08	0.5–100	0.9966	3.2	77	541
Haloxypop-etotyl	13.48	0.07	0.5–100	0.9947	4.3	82	576
Fenoxypop-P-ethyl	15.30	0.06	0.5–100	0.9980	2.4	63	443

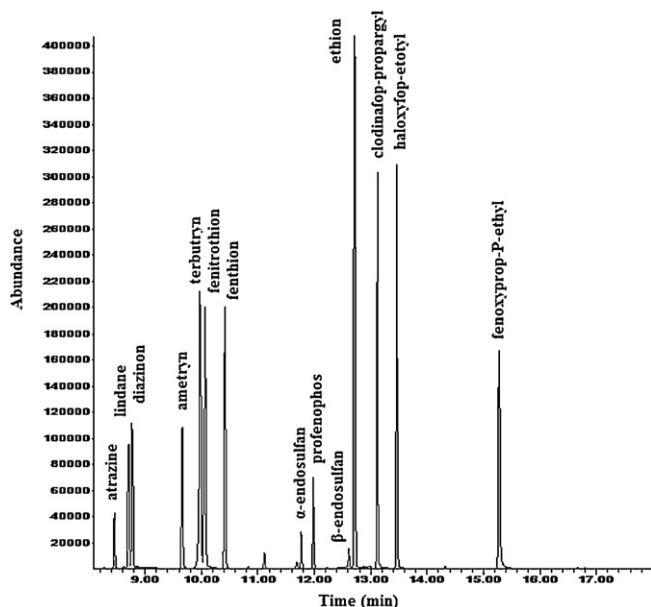


Fig. 8. Mass chromatogram obtained after extraction of selected pesticides from spiked Zayandeh-roud river water sample (5 ng mL^{-1}).

Gezel-ouzan river and Aydoghmoush river (East Azarbaijan province-Iran) were analyzed. First, all of samples were analyzed under optimum condition and no analyte was determined in these real samples. Then the spiked river water samples at 5 ng mL^{-1} were considered for this investigation. The obtained chromatogram for Zayandeh roud river water sample is illustrated in Fig. 8. Eventually, a matrix factor (MF) was calculated from the responses (R) of the analytes in the spiked and original sample as:

$$\text{MF} = \frac{[R_{\text{spiked river}} - R_{\text{non-spiked river}}]}{[R_{\text{spiked DW}}]}$$

The matrix factors listed in Table 4 are indication of the matrix influence extension on the analyte response in the MEPS–GC–MS analysis compared to the spiked double distilled water. The obtained MF is in the range of 0.88–1.04, 0.74–1.09 and 0.81–1.04 for Zayandeh roud river, Ghezel-ouzan river and Aydoghmoush river respectively. Apparently, the determination of all analytes was slightly affected by the river water matrix.

Table 4
Matrix factor obtained for different real samples.

Compound	Zayandeh roud river	Ghezel-ouzan river	Aydoghmoush river
Atrazine	1.02	0.74	0.91
Lindane	0.92	1.06	1.04
Diazinon	0.88	0.85	0.97
Ametryn	1.05	0.81	0.86
Terbutryn	0.98	0.82	0.83
Fenitrothion	0.92	0.89	0.96
Fenthion	0.92	0.88	0.97
α -Endosulfan	0.90	1.02	1.00
Profenophos	0.99	0.90	0.98
β -Endosulfan	0.89	0.99	0.97
Ethion	1.04	1.09	0.99
Clodinafop-propargyl	1.04	0.74	0.90
Haloxyfop-etotyl	1.06	0.82	0.81
Fenoxypop-P-ethyl	1.01	0.86	0.87

4. Conclusion

The PDPA/CNT nanocomposites containing different doping levels of CNTs were synthesized and their extraction capability was investigated. The results revealed that the synergic effect of the nanocomposites is significantly dependent on the doping level of CNT and the analytes structures. It was also shown that the CNT doping level of 6 mg (4%, w/w) has been led to higher synergic effect and therefore higher extraction capability. The doped CNTs in PDPA provide higher specific surface and increased loading capacity. The addition of CTAB in the polymerization mixture was led to highly CNTs dispersion and effective reinforcement of the synthesized polymer. The sample matrix has no significant effect as far as the river water sample is concerned. The analytical performance parameters such as recoveries, repeatability and robustness make the developed method excellently suited for the analysis of pollutants and pesticides in real aquatic media.

Acknowledgements

The Research Council and Graduate School of Sharif University of Technology (SUT) are acknowledged for supporting this project. Also, we would like to acknowledge the Iran National Elite Foundation for their support for Zahra Ayazi.

References

- [1] P.M. Ajayan, L.S. Schadler, P.V. Braun, Nanocomposite Science and Technology, Wiley-VCH, Weinheim, 2003.
- [2] E.T. Thostenson, C. Li, T.W. Chou, Compos. Sci. Technol. 65 (2005) 491.
- [3] J. Chen, M.A. Hamon, H. Hu, Y. Chen, A.M. Rao, P.C. Eklund, Science 282 (1998) 95.
- [4] O. Breuer, U. Sundararaj, Polym. Compos. 25 (2004) 630.
- [5] Z. Yang, X. Chen, C. Chen, W. Li, H. Zhang, L. Xu, Polym. Compos. 28 (2007) 36.
- [6] A.B. Dalton, C. Stephan, J.N. Coleman, B. McCarthy, P.M. Ajayan, S. Lefrant, J. Phys. Chem. B 104 (2000) 10012.
- [7] I. Szeleifera, R.Y. Rozen, Polymer 46 (2005) 7803.
- [8] X.B. Xu, Z.M. Li, L. Shi, X.C. Bian, Z.D. Xiang, Small 3 (2007) 408.
- [9] A.M. Showkat, K.P. Lee, A.I. Gopalan, S.H. Kim, S.H. Choi, S.H. Sohn, J. Appl. Polym. Sci. 101 (2006) 3721.
- [10] M. Wu, G.A. Snook, V. Gupta, M. Shaffer, D.J. Fray, G.Z. Chen, J. Mater. Chem. 5 (2005) 2297.
- [11] A. Star, J.F. Stoddart, D. Steuerman, M. Diehl, A. Boukai, E.W. Wong, Angew. Chem. Int. Ed. 40 (2001) 1721.
- [12] J.N. Coleman, S. Curran, A.B. Dalton, A.P. Davey, B. McCarthy, W. Blau, Synth. Met. 2 (1999) 1174.
- [13] E. Kymakis, G.A. Amaratunga, Appl. Phys. Lett. 80 (2002) 112.
- [14] J. Janata, M. Josowicz, Nat. Mater. 2 (2003) 19.
- [15] K. Ramanathan, M.A. Bangar, M. Yun, W. Chen, A. Mulchandani, N.V. Myung, Nano Lett. 4 (2004) 1237.
- [16] H. Bagheri, A. Mohammadi, A. Salemi, Anal. Chim. Acta 513 (2004) 445.
- [17] H. Bagheri, A. Mohammadi, J. Chromatogr. A 1015 (2003) 23.
- [18] Y. Yang, Y. Jiang, J. Xu, H. Yu, Polymer 48 (2007) 4459.
- [19] H. Bagheri, A. Mir, E. Babanezhad, Anal. Chim. Acta 532 (2005) 89.
- [20] H. Bagheri, M. Saraji, J. Chromatogr. A 986 (2003) 111.
- [21] H. Bagheri, E. Babanezhad, F. Khalilian, Anal. Chim. Acta 634 (2009) 209.
- [22] H. Bagheri, A. Aghakhani, M. Akbari, Z. Ayazi, Anal. Bioanal. Chem. 400 (2011) 3607.
- [23] Y.T. Tsai, T.C. Wen, A. Gopalan, Sensor Actuat. B 96 (2003) 646.
- [24] K. Suganandam, P. Santhosh, M. Sankarasubramanian, A. Gopalan, T. Vasudevan, K.P. Lee, Sensor Actuat. B 105 (2005) 223.
- [25] C. Jeyaprabha, S. Sathiyarayanan, K.L.N. Phani, G. Venkatachari, J. Electroanal. Chem. 585 (2005) 250.
- [26] P. Santhosh, A. Gopalan, T. Vasudevan, K.P. Lee, Appl. Surf. Sci. 252 (2006) 7964.
- [27] M. Abdel-Rehim, J. Chromatogr. A 1217 (2010) 2569.
- [28] M. Abdel-Rehim, Z. Altun, L. Blomberg, J. Mass Spectrom. 39 (2004) 1488.
- [29] Z. Altun, M. Abdel-Rehim, L.G. Blomberg, J. Chromatogr. B 813 (2004) 129.
- [30] A. El-Beqqali, A. Kussak, M. Abdel-Rehim, J. Chromatogr. A 1114 (2006) 234.
- [31] M. Abdel-Rehim, M. Dahlgren, S. Claude, R. Tabacchi, L. Blomberg, J. Liq. Chromatogr. Relat. Technol. 29 (2006) 2537.
- [32] M. Abdel-Rehim, J. Chromatogr. A 801 (2004) 317.
- [33] A. Prieto, S. Schrader, M. Moeder, J. Chromatogr. A 1217 (2010) 6002.
- [34] H. Bagheri, Z. Ayazi, Anal. Methods 3 (2011) 2630.
- [35] Y.S. Song, J.R. Youn, Carbon 43 (2005) 1378.
- [36] J.B. Bai, A. Allaoui, Compos. Part A 34 (2005) 689.
- [37] D. Qian, E.C. Dickey, R. Andrews, T. Rantell, Appl. Phys. Lett. 76 (2000) 2868.
- [38] C. Park, Chem. Phys. Lett. 364 (2002) 303.

- [39] H.T. Ham, Y.S. Choi, J.I. Chung, J. Colloid Interf. Sci. 286 (1) (2005) 216.
- [40] J.P. Salvetat, A.D. Briggs, J.M. Bonard, R.R. Bacsa, A.J. Kulik, T. Stockli, Phys. Rev. Lett. 82 (5) (1999) 944.
- [41] X. Gong, J. Liu, S. Baskaran, Chem. Mater. 12 (2000) 1049.
- [42] Z. Chan, F. Miao, Z. Xiao, H. Juan, Z. Hongbing, Mater. Lett. 61 (2007) 644.
- [43] K. Gong, M. Zhang, Y. Yan, L. Su, L. Mao, S. Xiong, Y. Chen, Anal. Chem. 76 (2004) 6500.
- [44] H. Bagheri, Z. Ayazi, A. Aghakhani, Anal. Chim. Acta 683 (2011) 212.
- [45] S.L. Cockroft, J. Perkins, C. Zonta, H. Adams, S.E. Spey, C.M.R. Low, J.G. Vinter, K.R. Lawson, C.J. Urch, C.A. Hunter, Org. Biomol. Chem. 5 (2007) 1062.
- [46] C.A. Hunter, J.K.M. Sanders, J. Am. Chem. Soc. 112 (1990) 5525.
- [47] F. Tournus, S. Latil, M.I. Heggie, J.C. Charlier, Phys. Rev. B 72 (2005) 075431.
- [48] L.M. Woods, S.C. Badescu, T.L. Reinecke, Phys. Rev. B 75 (2007) 155415.
- [49] A. Star, T.R. Han, J.C.P. Gabriel, K. Bradley, G. Grüner, Nano Lett. 3 (2003) 1421.
- [50] K. Yang, W.H. Wu, Q.F. Jing, L.Z. Zhu, Environ. Sci. Technol. 42 (2008) 7931.
- [51] L.G. Blomberg, Anal. Bioanal. Chem. 393 (2009) 797.